A case study of energy absorption buildup factors in some human bones for gamma energies 30 keV to 1.5 MeV

Vishwanath P Singh[1], Seyed Pezhman Shirmardi*[2], Reza Bagheri[3], RuhollahAdeli[4], Mansoureh Tatari[5]

[1]Department of Physics, Karnataka University, Dharwad, India
[2]Radiation Application Research School, Nuclear Science and Technology Research Institute (NSTRI), Tehran, Iran
[3] Reactor School, Nuclear Science & Technology Research Institute (NSTRI), Tehran, Iran
[4]Nuclear Fuel Cycle Research School, Nuclear Science and Technology Research Institute (NSTRI), Tehran, Iran
[5]Physics Department, Yazd University, Iran

[*]Corresponding author: email address: pshirmardi@aeoi.org.ir (P.Shirmardi)

ABSTRACT

Human body consists of some tissues which bone is one of the important living and growing tissues. In this research, energy absorption buildup factor (EABF) values of 27 types of bone have been computed for photon energy 0.03 to 1.5 MeV up to 40 mean free path (40mfp) penetration depths. The Inner bone tissue, Spongiosa and Male sternum had the largest values of EABF in low photon energies, and great differences below 150 keV photon energy were noted relative to the other bones. This study would be of utmost importance for estimation of the effective dose to the human bones, radiation therapy and various medical applications.

Keywords: Energy absorption buildup factor; GP fitting; Bone; Photon

INTRODUCTION

The effect of radiation on human organs depends upon absorbed dose, energy, radiation types and organs irradiated. Gamma and x-rays have various interactions with the materials (Photo electric absorption, Compton scattering, Pair production and Coherent) [1-13]. These photons colliding the human organs not only loose energy and are absorbed, but also generate new photons by multiple scattering [2,3,12]. Buildup factor is an enhancing factor used to get the corrected response to un-collided photons by including the contribution of scattered photons. This factor depends upon the energy of the photons, atomic number of the target and the penetration depth, as well as the radiation source and the medium geometry. The buildup factor in which the quantity of interest is the absorbed energy in the medium is defined as the energy absorption buildup factor. In 1993, Harima prepared a review on calculations and applications of buildup factors [10]. In medical applications, photons (Gamma- and X-rays) are mostly used for radiotherapy and diagnostic of a lot of diseases [12]. As a result, different body tissues are being exposed to photons. Therefore, having the data about how these radiations interact with the body is an essential piece of information. When gamma or x-rays enter the body, they reduce their energy inside the body, leading to secondary photon which can be estimated by buildup factor. Owing to the buildup of degraded gamma rays by scattering within the tissue, the maximum dose to the tissue is located at the inside when tissues are exposed to radiations. Considering the importance of buildup of scattered gamma rays, an attempt has been made to calculate the EABF for some bones. Lately, buildup factors for some polymers and tissue substitute materials were computed by Kurudirek and coworkers [12]. There is a need for gamma-ray buildup factors of low-Z complex materials, such as various bones, in radiotherapy and diagnostics for dose estimations. In general, the results of the study can help in estimating safe dose levels for radiotherapy and diagnostics. In the present study, we have calculated energy absorption buildup factors (EABF) for various bones, such as inner bone tissue, Spongiosa and Male sternum, etc. The calculations have been performed for energies of 30keV–1.5 MeV up to penetration depths of 40 mean free paths. The produced buildup factor data is studied as a function of incident photon energy, etc. The data will be helpful for many applications especially in radiotherapy and diagnostic, for the preparation of phantoms using bone-equivalent materials.

MATERIALS AND METHODS

Elemental compositions of different bones in human body are seen in Table 1 [14]. The Z_{eq} of the bone tissues for interactions varies with the energy of photons. The buildup of photons in the materials is more due to Compton scattering, so Z_{eq} is derived from the Compton scattering process.

The buildup factors of bones are estimated by using GP fitting coefficients in the gamma energies up to 40 mfp using the equations [1-3, 9-11] given below,

$$B(E,x)=\begin{cases}1+\dfrac{(b-1)(K^{x}-1)}{K-1} & \text{for } K\neq 1\\ 1+(b-1)x & \text{for } K=1\end{cases} \tag{1}$$

$$K(E,x)=cx^{a}+d\frac{\tanh(x/X_K-2)-\tanh(-2)}{1-\tanh(-2)} \quad \text{for } x\leq 40\text{ mfp} \tag{2}$$

where E is the energy of source, x is the penetration depth in units of mfp (mean free path), and a, b, c, d and X_k are GP fitting parameters. The value of the parameter b represents the buildup factor at 1 mfp. The variation of the parameter K with penetration depth corresponds to the photon dose multiplication.

Table 1. Elemental composition of some bones [14].

Sample Name	Density	H	C	N	O	Na	Mg	P	S	Cl	K	Ca	Fe
Inner bone tissue	**1.12**	**8.680**	**13.014**	**3.604**	**66.473**	**0.080**	**0.06**	**2.433**	**0.461**	**0.000**	**0.230**	**4.965**	**0.000**
Spongiosa	**1.18**	**8.556**	**29.090**	**2.380**	**48.434**	**0.079**	**3.232**	**0.139**	**0.456**	**0.000**	**0.228**	**7.406**	**0.000**
Male stemum	**1.25**	**7.799**	**31.686**	**3.615**	**44.148**	**0.050**	**0.080**	**3.964**	**0.120**	**0.000**	**0.110**	**8.378**	**0.050**
Sacrum Male	**1.29**	**7.403**	**30.240**	**3.646**	**44.156**	**0.050**	**0.090**	**4.525**	**0.130**	**0.000**	**0.100**	**9.620**	**0.040**
D6L3 male with cartilage	**1.30**	**7.308**	**26.677**	**3.519**	**47.759**	**0.040**	**0.090**	**4.541**	**0.241**	**0.000**	**0.080**	**9.704**	**0.040**
Famur whole column	**1.32**	**7.089**	**25.960**	**3.540**	**47.669**	**0.040**	**0.100**	**4.853**	**0.241**	**0.000**	**0.080**	**10.398**	**0.030**
Male vertebral column	**1.33**	**7.098**	**25.792**	**3.599**	**47.186**	**0.100**	**0.100**	**5.098**	**0.300**	**0.100**	**0.100**	**10.497**	**0.030**
D6L3 male no cartilage	**1.33**	**6.987**	**28.706**	**3.673**	**44.106**	**0.050**	**0.100**	**5.100**	**0.150**	**0.100**	**0.090**	**10.899**	**0.040**
Humerus spherical head	**1.33**	**7.084**	**37.813**	**2.594**	**34.122**	**0.100**	**0.100**	**5.587**	**0.200**	**0.100**	**0.090**	**12.172**	**0.040**
Famur spherical head	**1.34**	**6.941**	**24.873**	**2.892**	**47.213**	**0.020**	**0.070**	**5.455**	**0.189**	**0.100**	**0.090**	**12.117**	**0.040**
C4 male with cartilage	**1.37**	**6.645**	**24.456**	**3.578**	**47.519**	**0.050**	**0.050**	**5.473**	**0.261**	**0.100**	**0.070**	**11.767**	**0.030**
Famur conical traochanter	**1.37**	**6.735**	**24.314**	**2.953**	**47.032**	**0.020**	**0.080**	**5.737**	**0.200**	**0.100**	**0.070**	**12.731**	**0.030**
Secrum female	**1.38**	**6.547**	**27.086**	**3.713**	**44.092**	**0.050**	**0.120**	**5.729**	**0.170**	**0.100**	**0.080**	**12.275**	**0.040**
Humerus whole specimen	**1.39**	**6.514**	**23.743**	**3.023**	**46.838**	**0.020**	**0.080**	**6.026**	**0.209**	**0.100**	**0.080**	**13.328**	**0.040**
Male ribs 2 and 6	**1.41**	**6.3**	**26.33**	**3.72**	**44.10**	**0.05**	**0.12**	**6.020**	**0.18**	**0.10**	**0.08**	**12.91**	**0.03**

		39	5	4	5	0	0		0	0	0	8	0
Male pelvic bones	**1.41**	**6.330**	**26.288**	**3.724**	**44.099**	**0.050**	**0.120**	**6.040**	**0.180**	**0.100**	**0.070**	**12.969**	**0.030**
C4 male no cartilage	**1.42**	**6.280**	**26.108**	**3.734**	**44.099**	**0.050**	**0.120**	**6.110**	**0.180**	**0.100**	**0.070**	**13.119**	**0.030**
Famur whole specimen	**1.43**	**6.176**	**22.840**	**3.123**	**46.538**	**0.030**	**0.100**	**6.476**	**0.220**	**0.100**	**0.070**	**14.299**	**0.030**
Female pelvic bones	**1.45**	**5.980**	**25.010**	**3.754**	**44.099**	**0.050**	**0.130**	**6.530**	**0.200**	**0.100**	**0.070**	**14.048**	**0.030**
Humerus total bone	**1.46**	**6.004**	**31.279**	**2.902**	**37.312**	**0.040**	**0.140**	**6.894**	**0.230**	**0.100**	**0.070**	**14.999**	**0.030**
Male clavicle scapula	**1.46**	**5.994**	**31.232**	**2.902**	**37.336**	**0.040**	**0.140**	**6.905**	**0.230**	**0.100**	**0.070**	**15.021**	**0.030**
Humerus cylindrical shaft	**1.49**	**5.719**	**21.627**	**3.263**	**46.128**	**0.030**	**0.120**	**7.086**	**0.230**	**0.100**	**0.070**	**15.599**	**0.030**
Male ribs 10	**1.51**	**5.569**	**23.493**	**3.782**	**44.072**	**0.050**	**0.150**	**7.126**	**0.210**	**0.100**	**0.080**	**15.329**	**0.040**
Cranium	**1.60**	**4.934**	**21.195**	**3.845**	**44.087**	**0.060**	**0.160**	**8.000**	**0.240**	**0.100**	**0.040**	**17.319**	**0.020**
Mandible	**1.66**	**4.586**	**19.892**	**3.867**	**44.090**	**0.060**	**0.170**	**8.502**	**0.260**	**0.100**	**0.030**	**18.433**	**0.010**
Femur culindrical shaft	**1.75**	**4.194**	**20.372**	**3.795**	**41.442**	**0.100**	**0.200**	**9.287**	**0.300**	**0.100**	**0.030**	**20.172**	**0.010**
Cortical bone	**1.90**	**3.387**	**15.488**	**3.967**	**44.065**	**0.060**	**0.210**	**10.192**	**0.310**	**0.100**	**0.030**	**22.182**	**0.010**

RESULTS AND DISCUSSION

Figures (2-6) show the results of EABF for bones at selected energies (Figure 1(a -g)) as well as at different penetration depths. Also the variation of EABF with the some bones at different energies and penetration depth (Figure 7(a-e)) has been shown in graphical form. As shown in figure 1(a-g), it has been indicated that EABF values of bones start increasing with increase in gamma energy up to a maximum value at around 100-150keV. Due to the photoelectric absorption, more increase in gamma energy decreases the value of EABF. With increase in gamma energy the Compton scattering process is dominant which results in more multiple scattering and leads to increase in EABF values. Maximum values of EABF for all bones have been observed at 150keV figure1 (a-g). In high energies (>1MeV), the variation of EABF with incident gamma energy seems to be independent of the chemical composition of given samples at this energy region.

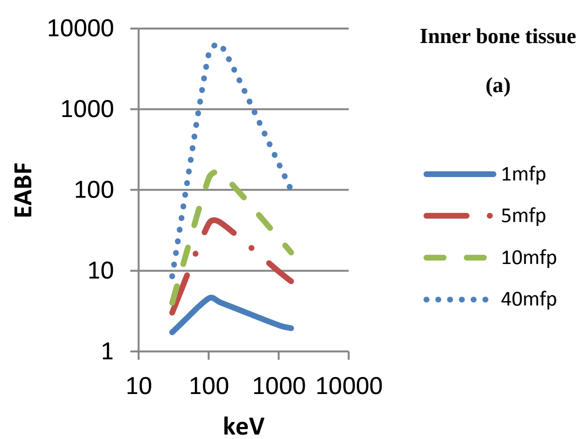

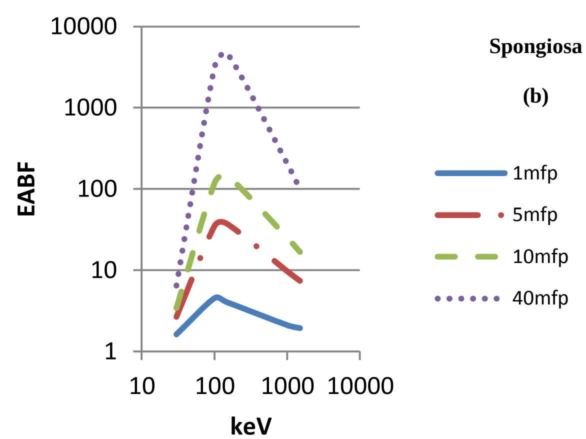

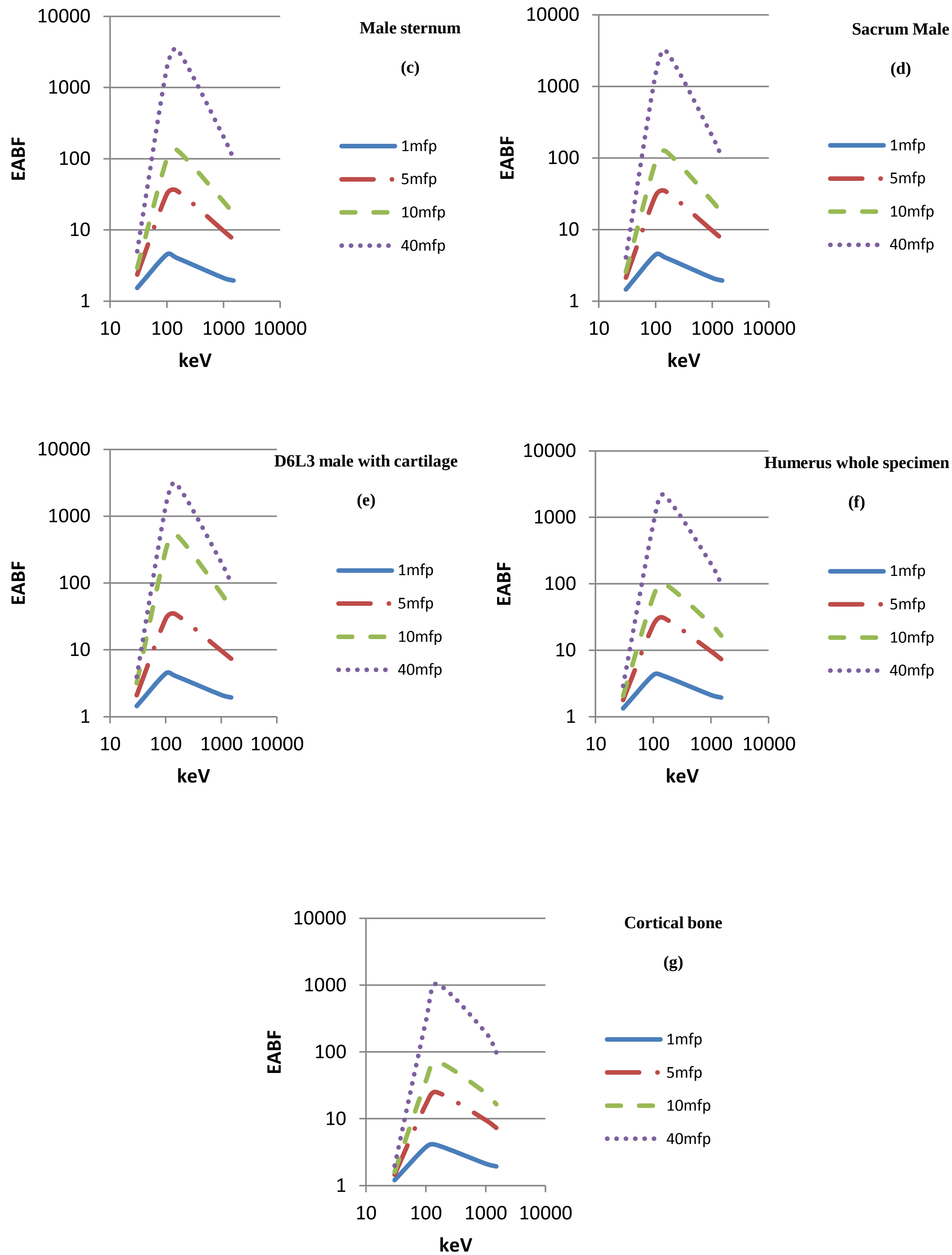

Figure 1. Variation of EABF as a function of incident photon energy (keV) for Inner bone tissue, spongiosa, mal sternum , sacrum male, D6L3 male with cartilage, Humerus whole specimen And cortical bone.

The curves at different energies in figures (2-6) show that there is increase in EABF with increase in penetration depth for all samples. It is due to the fact that the increase in penetration depth increases the interaction of gamma-radiation photons with matter resulting in generation of large number of low energy photons due to occurrence of Compton scattering process. It has been observed that at lower than 100keVenergies the values of EABF for the bones is low and the variation is between 2-9 for 40 mfp. By increasing the energy to 100-150keV, EABF increases to higher than 6000 for 40 mfp. The variation in this range of energies will be more severe. The variation of EABF in low penetration depth is not affected by the type of bone samples. In the energy range of 1-1.5MeV, EABF has the almost constant values for lower mfp (lower 10mfp), and increases to higher than 200 for 40 mfp. The EABF in high energies is not affected by the chemical composition; so, in the medium gamma energies, EABF has the maximum values for all bones, and in low energies has the minimum values. It is shown that for energies higher than1MeV, there is a drop in the value of EABF which ultimately indicates the dominance of pair production process in this range of energy.

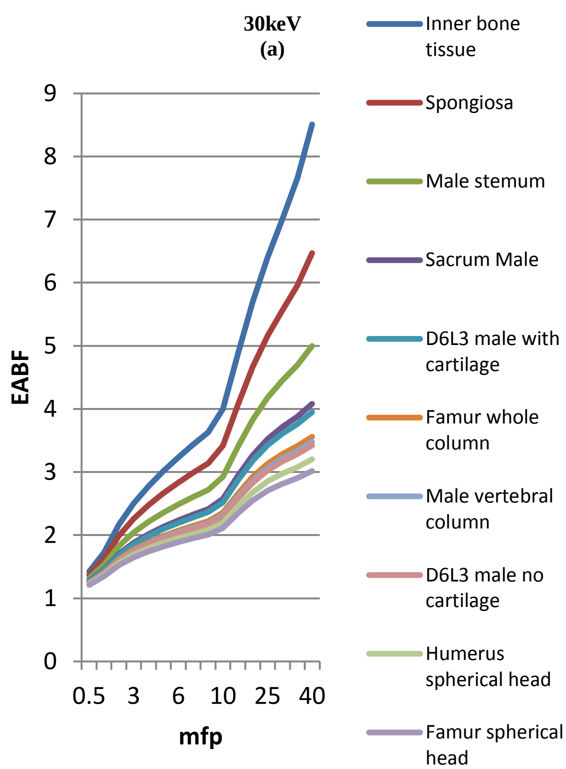

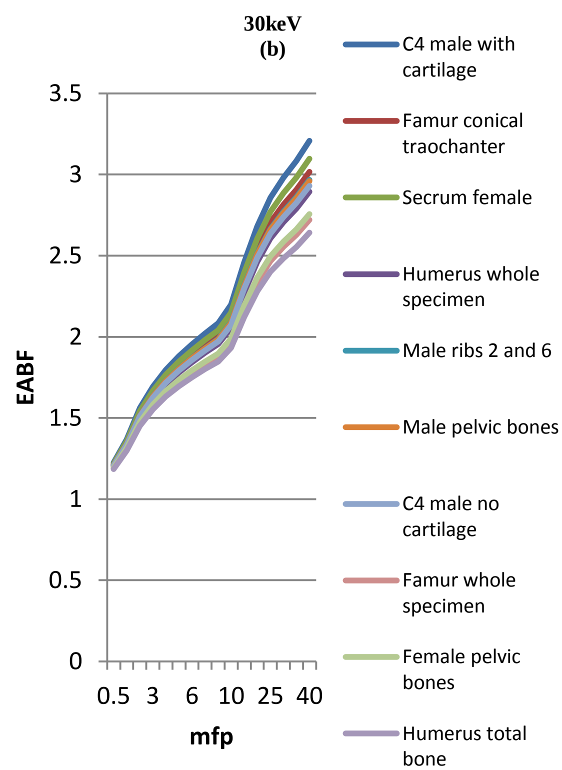

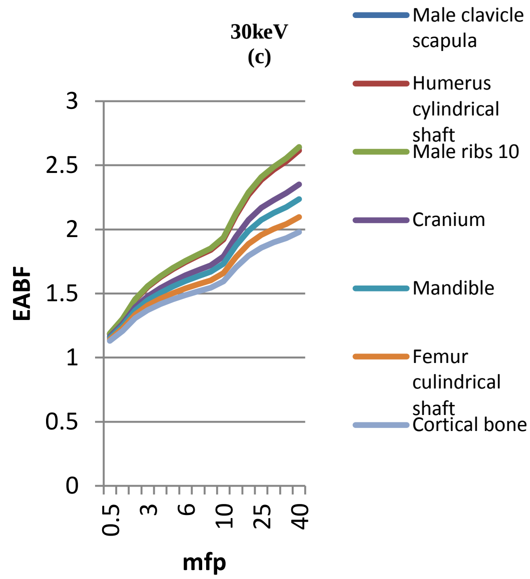

Figure 2. Variation of EABF with penetration depth of all bones at energy 30keV

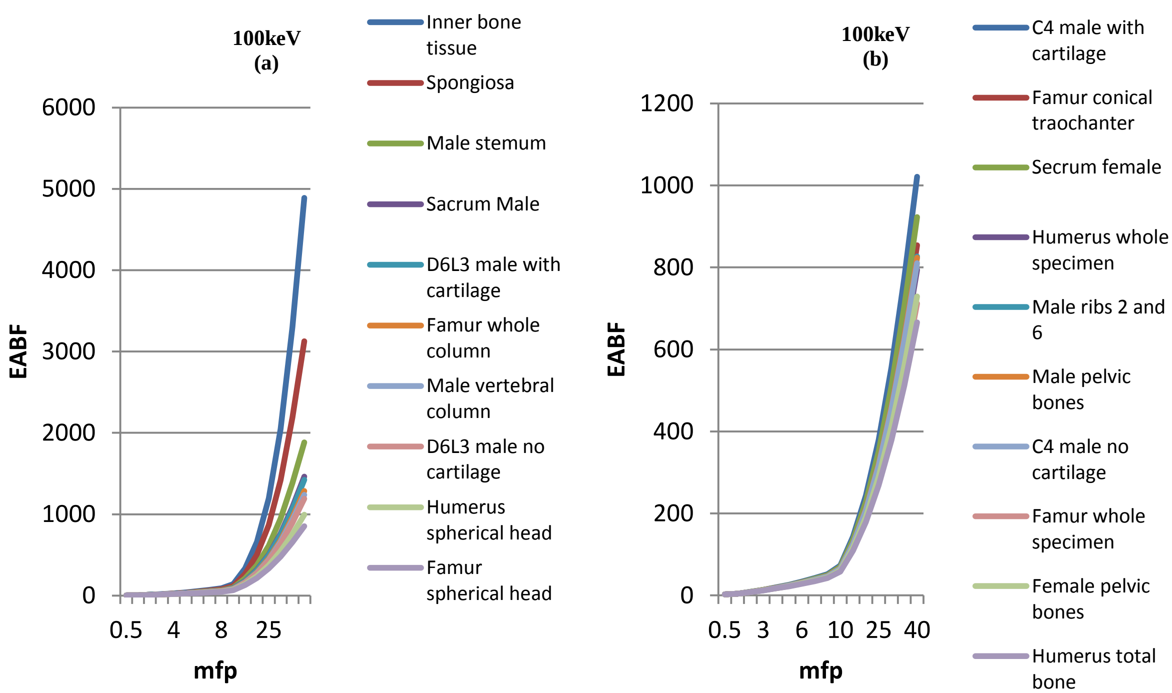

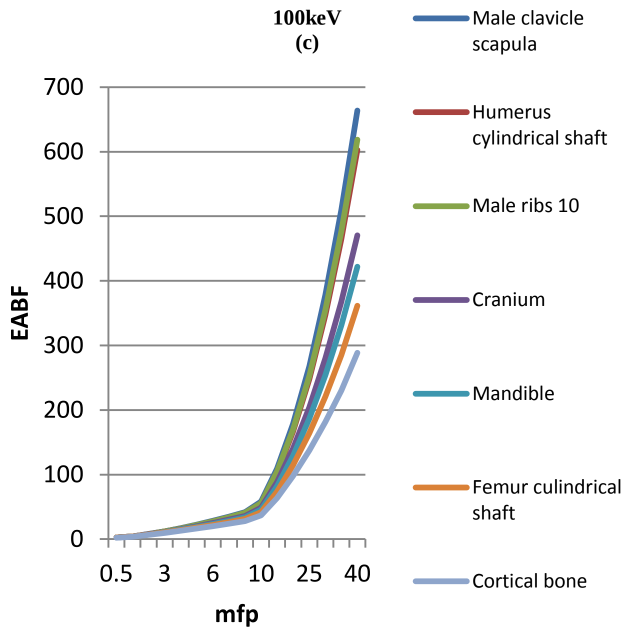

Figure 3. Variation of EABF with penetration depth of all bones at energy 100keV

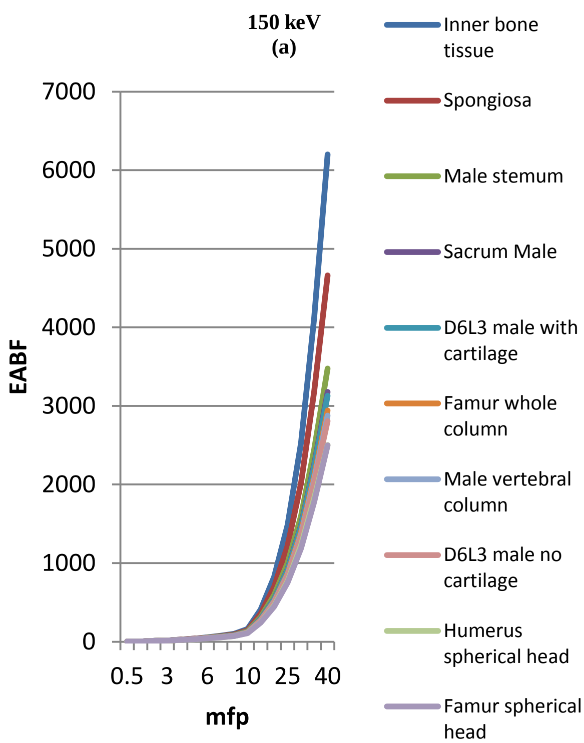

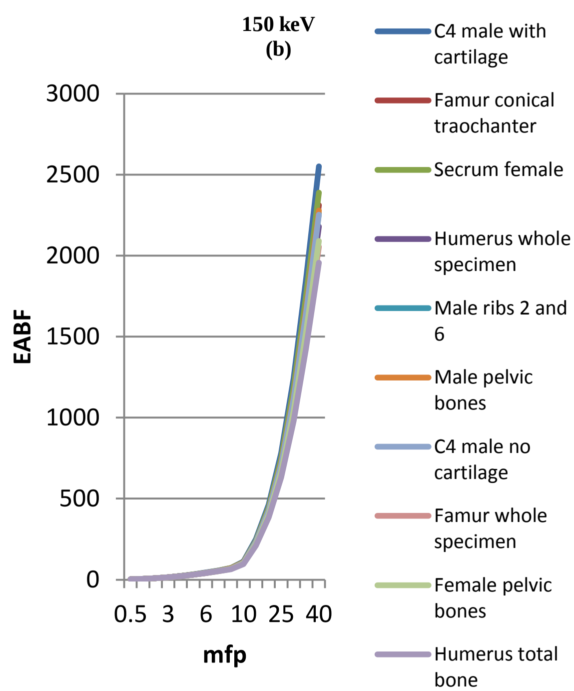

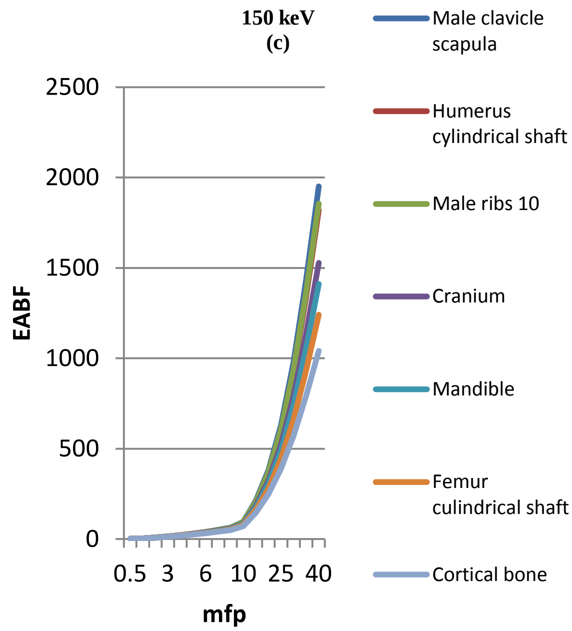

Figure 4. Variation of EABF with penetration depth of all bones at energy 150keV

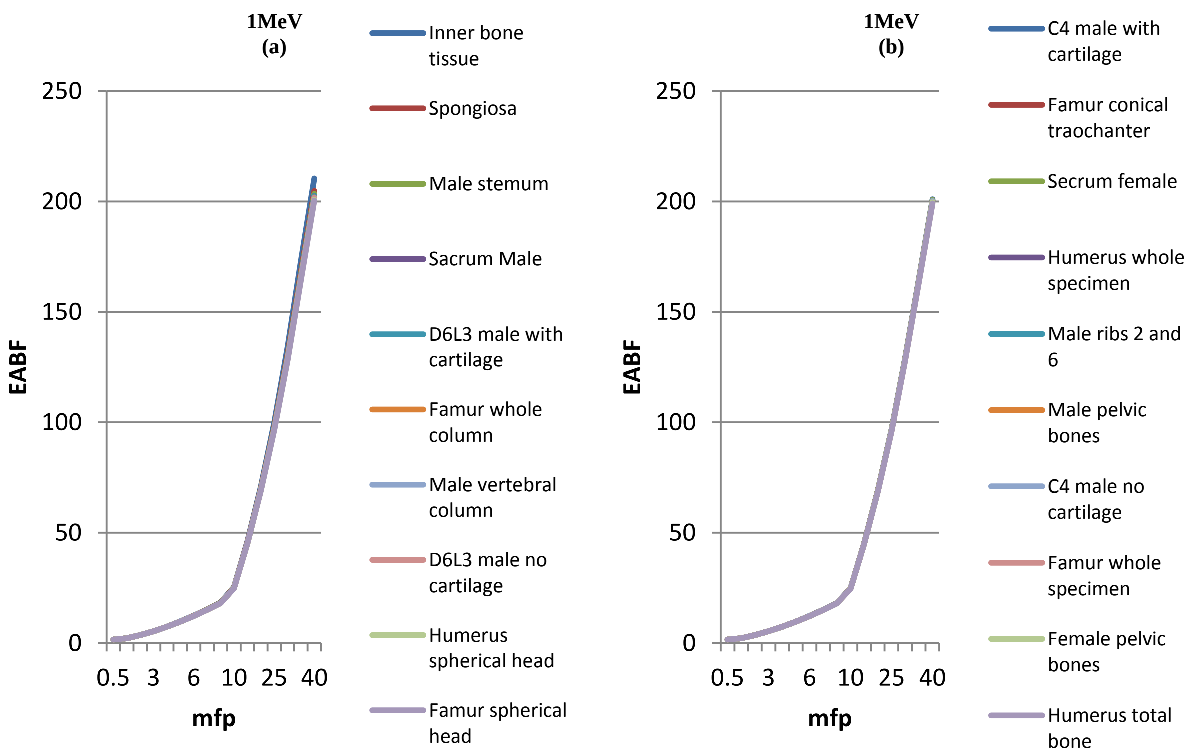

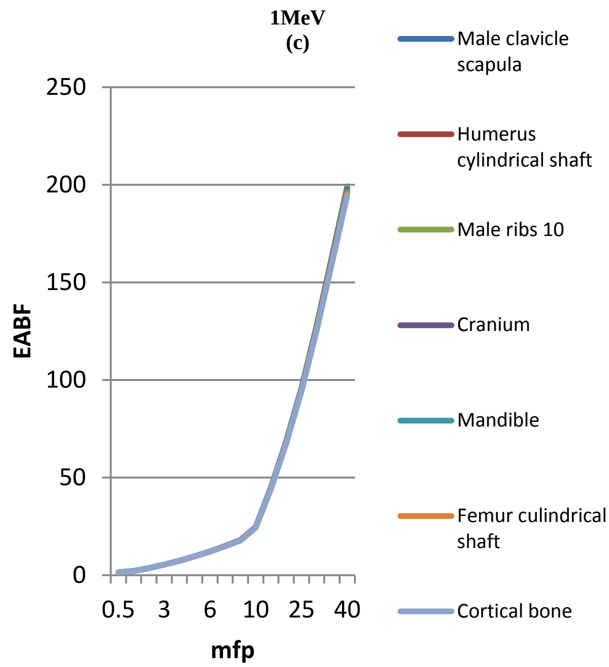

Figure 5. Variation of EABF with penetration depth of all bones at energy 1MeV

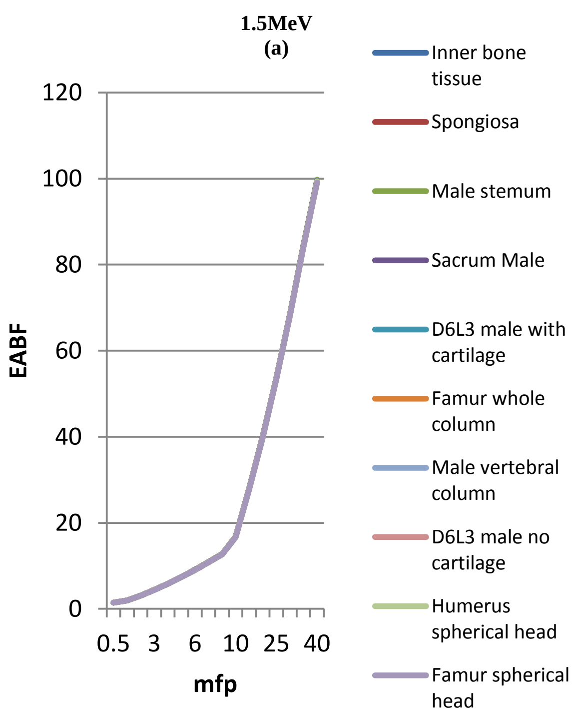

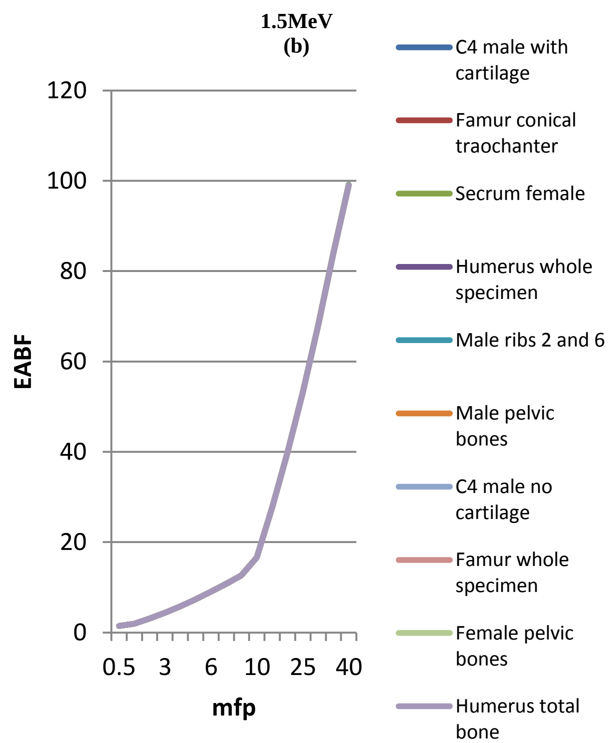

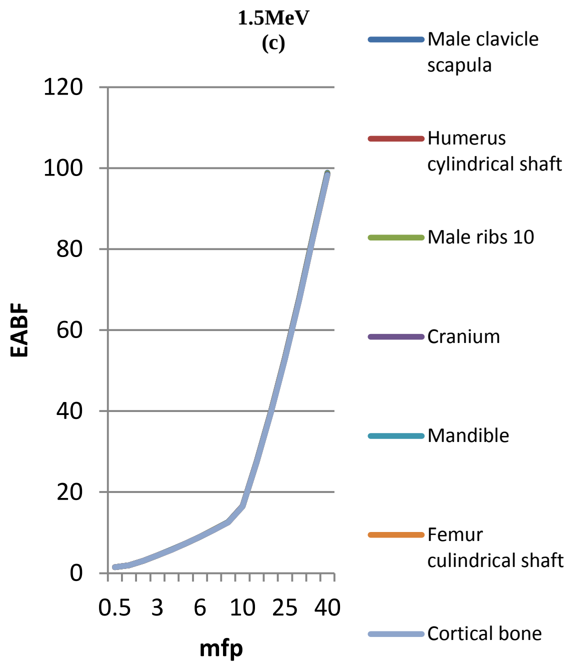

Figure 6. Variation of EABF with penetration depth of all bones at energy 1.5MeV

The results show that with the increase in energy, EABF for all bones got constant values. Therefore,, the curves are straight lines in 1.5 MeV.

EABF values for bones with lower density such as inner bone tissue, spongiosa and male sternum are the maximum in low energies (30keV) relative to the other bones.

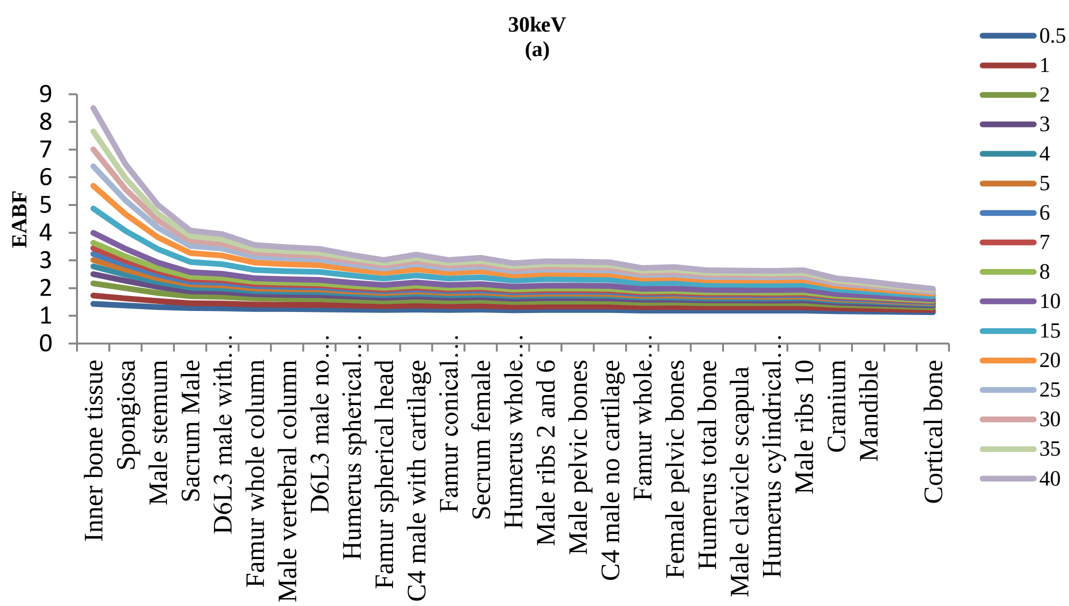

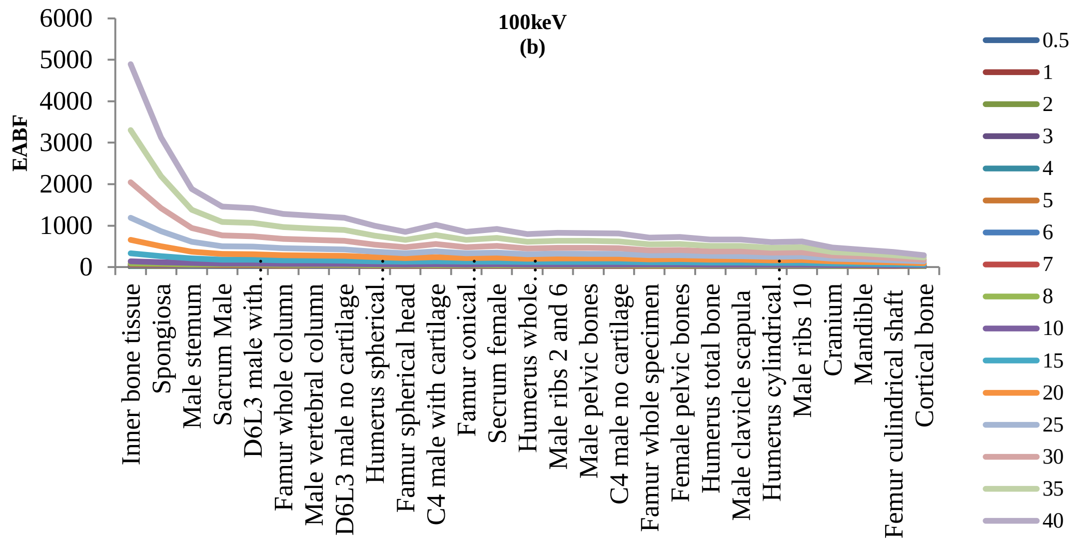
100keV
(b)
EABF
6000
5000
4000
3000
2000
1000
0
Inner bone tissue
Spongiosa
Male stemum
Sacrum Male
D6L3 male with...
Famur whole column
Male vertebral column
D6L3 male no cartilage
Humerus spherical...
Famur spherical head
C4 male with cartilage
Famur conical...
Secrum female
Humerus whole...
Male ribs 2 and 6
Male pelvic bones
C4 male no cartilage
Famur whole specimen
Female pelvic bones
Humerus total bone
Male clavicle scapula
Humerus cylindrical...
Male ribs 10
Cranium
Mandible
Femur culindrical shaft
Cortical bone
0.5
1
2
3
4
5
6
7
8
10
15
20
25
30
35
40

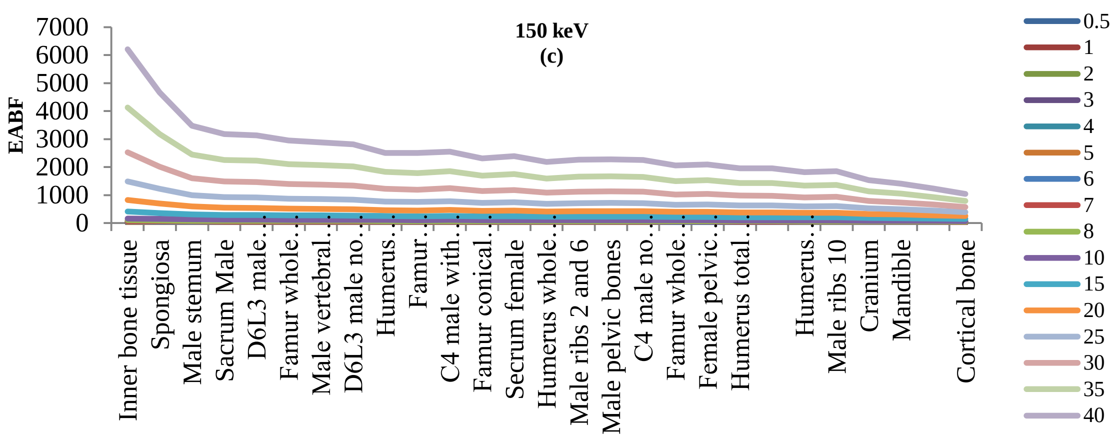
150 keV
(c)
EABF
7000
6000
5000
4000
3000
2000
1000
0
Inner bone tissue
Spongiosa
Male stemum
Sacrum Male
D6L3 male...
Famur whole...
Male vertebral...
D6L3 male no...
Humerus...
Famur...
C4 male with...
Famur conical...
Secrum female
Humerus whole...
Male ribs 2 and 6
Male pelvic bones
C4 male no...
Famur whole...
Female pelvic...
Humerus total...
Humerus...
Male ribs 10
Cranium
Mandible
Cortical bone
0.5
1
2
3
4
5
6
7
8
10
15
20
25
30
35
40

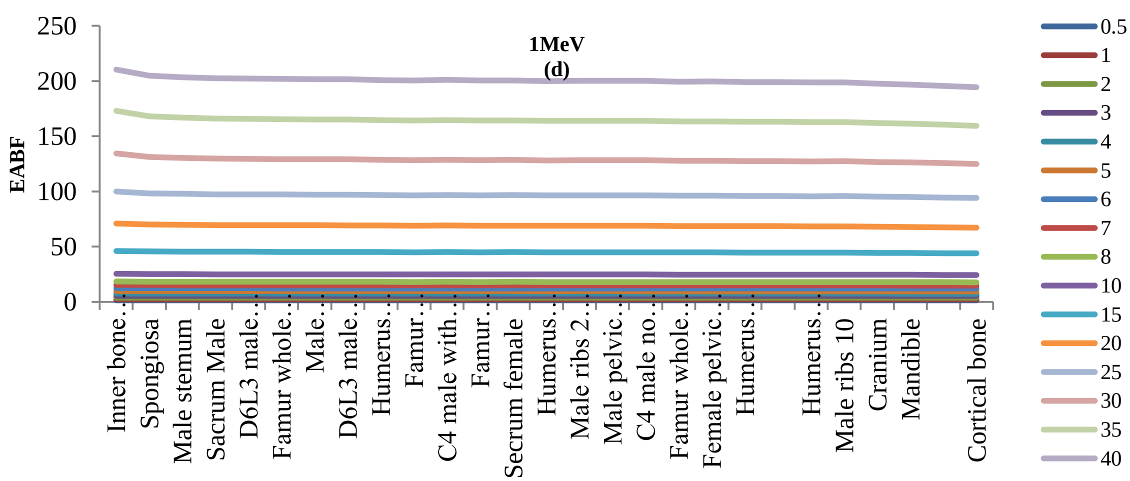
1MeV
(d)
EABF
250
200
150
100
50
0
Inner bone...
Spongiosa
Male stemum
Sacrum Male
D6L3 male...
Famur whole...
Male...
D6L3 male...
Humerus...
Famur...
C4 male with...
Famur...
Secrum female
Humerus...
Male ribs 2...
Male pelvic...
C4 male no...
Famur whole...
Female pelvic...
Humerus...
Humerus...
Male ribs 10
Cranium
Mandible
Cortical bone
0.5
1
2
3
4
5
6
7
8
10
15
20
25
30
35
40

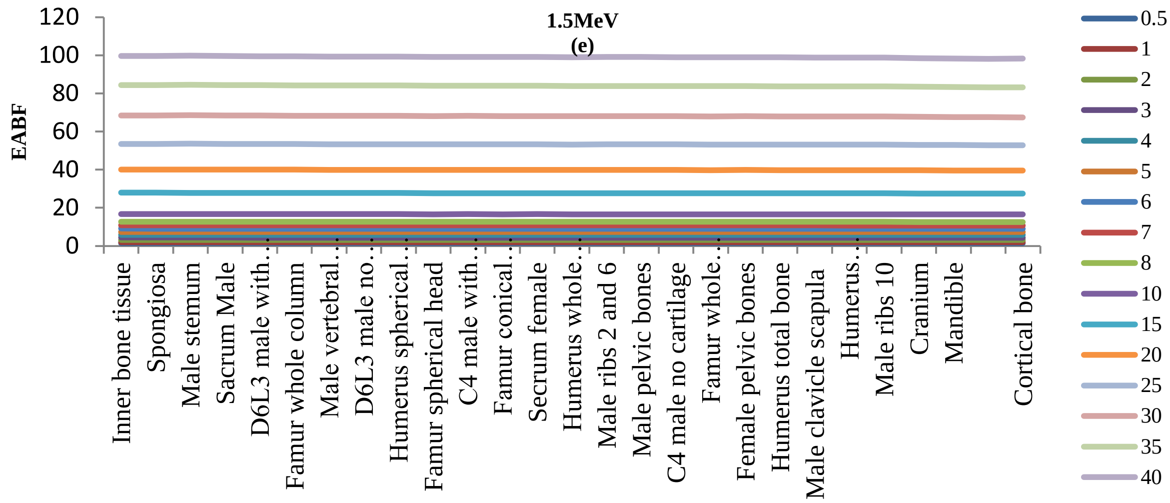

Figure 7. (a-e).Variation of EABF with the kinds of bones at different energies and mfps.

Generally, the EABF is small for all depths of penetration (mfp) at low energies. Photoelectric is the conquering gamma interaction process at low energies, leading to an exclusion of the incident of low-energy gamma rays and thus not allowing any tangible buildup of gamma rays. The EABF got large values at range of energies 100-150keV; at this range of energy the interaction cross sections for Compton scattering is high and the EABF reaches large values for a given penetration depth. This is owed to the multiple scattering of gamma rays in Compton scattering. The multiple scattered gamma rays exist for a longer time in the material, which results in a higher value of buildup factor.

CONCLUSION

In this research, the energy absorption buildup factor (EABF) values of different bones in energy range 30keV to 1.5 MeV up to 40 mfp penetration depths were calculated. The variation of EABF values of the bones proved to be dependent upon the photon energy, the penetration depth and the chemical compositions. According to the results, increase in gamma energy decreases the value of EABF,; moreover, in high mfp's, EABF has an enhancing state for all bone tissues increase (EABF variations are severe in above 8mfp). EABF variations for bone tissues are almost constant in high gamma energies. The bone equivalent and dosimetric properties of the present selected bone tissues are useful in clinical applications such as radiological examinations and therapeutic under radiation conditions where the effective energy of the photon attenuation field is difficult to assess.

ACKNOWLEDGEMENT

"The authors are thankful Dr. Roshanzamir for editing the paper. "

"The authors declare no conflict of interest"

REFERENCES

1. Singh SP, Singh T, Kaur P. Variation of energy absorption buildup factors with incident photon energy and penetration depth for some commonly used solvents. Ann Nucl Energy. 2008; 35:1093–1097.
2. Singh VP, Badiger NM. Comprehensive study on energy absorption buildup factors and exposure buildup factors for photon energy 0.015to 15 MeV up to 40 mfp penetration depth for gel dosimeters. Radiat Phys Chem. 2014b; 103:234–242.
3. Singh VP, Badiger NM. Energy absorption buildup factors, exposure buildup factors and Kerma for optically stimulated luminescence materials and their tissue equivalence for

radiation dosimetry. Radiat Phys Chem. 2014a; 104:61–67.
4. Shirmardi SP, Shamsaei M, Naserpour M, Comparison of photon attenuation coefficients of various barite concretes and lead by MCNP code, XCOM and experimental data, Annals of Nuclear Energy 2013; 55 :288–291.
5. ANSI/ANS-6.4.3. 1991. Gamma ray attenuation coefficient and buildup factors for engineering materials American Nuclear Society, La Grange Park, IL.
6. Shirmardi SP, Singh VP, Medhat ME, Adeli R and Saniei E, MCNP modeling of Attenuation Coefficients of Steel, Red brass, Pearl and Beryl in comparison with Experimental and XCOM data, J Nucl Ene Sci Power Generat Technol 2016; 5:2.
7. Singh VP, Medhat ME, Shirmardi SP, Comparative studies on shielding properties of some steel alloys using Geant4, MCNP, WinXCOM and experimental results, Radiation Physics and Chemistry. 2015; 106:255–260.
8. Esfandiari M, Shirmardi SP, Medhat ME, Element analysis and calculation of the attenuation coefficients for gold, bronze and water matrixes using MCNP, WinXCom and experimental data, Radiation Physics and Chemistry, 2014;99:30–36.
9. Harima Y. An approximation of gamma ray buildup factors by modified geometrical progression. Nucl Sci Eng. 1983; 830:299.
10. Harima Y. An historical review and current status of buildup factor calculations and applications. Radiat Phys Chem. 1993; 41:631–672.
11. Harima Y, Sakamoto Y, Tanaka S, Kawai M. Validity of the geometric-progression formula in approximating gamma ray buildup factors.Nucl Sci Eng. 1986;94:24–35.
12. Kurudirek M, Do˘gan B, Ingec M, Ekinci N, O¨zdemir YU, Gamma-ray energy absorption and exposure buildup factor studies in some human tissues with endometriosis, Applied Radiation and Isotopes. 2011; 69:381–388.
13. Asano Y, Sakamoto Y, 2007. Gamma ray buildup factors for heavy concretes. JAEData/Code 2007-006.
14. Zhou H, Keall PJ, Graves EE, A bone composition model for Monte Carlo x-ray transport simulations, Med. Phys. 2009; 36 (3), 1008-1018.